ELSEVIER

Biochimica et Biophysica Acta 1461 (1999) 155–173

BIOCHIMICA ET BIOPHYSICA ACTA
BBA

www.elsevier.com/locate/bba

Interactions of elastic and rigid vesicles with human skin in vitro: electron microscopy and two-photon excitation microscopy

Benedicte A.I. van den Bergh [a], Jurrien Vroom [b], Hans Gerritsen [b], Hans E. Junginger [a], Joke A. Bouwstra [a,*]

[a] *Department of Pharmaceutical Technology, Leiden Amsterdam Center for Drug Research, University of Leiden, P.O. Box 9502, 2300 RA Leiden, Netherlands*

[b] *Department of Molecular Biophysics, University of Utrecht, Utrecht, The Netherlands*

Received 18 January 1999; received in revised form 1 September 1999; accepted 15 September 1999

Abstract

Interactions between vesicle formulations and human skin were studied, in vitro, in relation to their composition and elasticity. The skin ultrastructure was investigated using transmission electron microscopy (TEM), freeze-fracture electron microscopy (FFEM) and two-photon fluorescence microscopy (TPE). The main difference between the vesicle formulations was their elasticity. Elastic vesicle formulations contained bilayer forming surfactants/lipids and single-chain surfactant octaoxyethylenelaurate-ester (PEG-8-L), whereas rigid vesicles contained bilayer surfactants in combination with cholesterol. TEM results showed three types of interactions after non-occlusive application of elastic PEG-8-L containing vesicle formulations on human skin: (1) the presence of spherical lipid structures containing or surrounded by electron dense spots; (2) oligolamellar vesicles were observed between the corneocytes in the upper part of the stratum corneum; and (3) large areas containing lipids, surfactants and electron dense spots were observed deeper down into the stratum corneum. Furthermore, after treatment with vesicles containing PEG-8-L and a saturated C12-chain surfactant, small stacks of bilayers were found in intercellular spaces of the stratum corneum. Rigid vesicles affected only the most apical corneocytes to some extent. FFEM observations supported the TEM findings. Major morphological changes in the intercellular lipid bilayer structure were only observed after treatment with PEG-8-L containing elastic vesicles. TPE showed a distinct difference in penetration pathways after non-occlusive application of elastic or rigid vesicles. After treatment with elastic vesicles, thread-like channels were formed within the entire stratum corneum and the polygonal cell shape of corneocytes could not be distinguished. Fluorescent label incorporated in rigid vesicles was confined to the intercellular spaces of the upper 2–5 μm of the stratum corneum and the cell contours could still be distinguished.

Keywords: Vesicle; Human skin; Topical application; Elasticity; Electron microscopy; Two-photon fluorescence microscopy

1. Introduction

The most superficial layer of the skin, the stratum corneum, constitutes the major physical barrier for most drugs. The stratum corneum is regarded as a heterogeneous two-compartment system composed of keratin-filled corneocytes, embedded in a lipid-en-

Abbreviations: PEG-8-L, octaoxyethylenelaurate-ester; L-595, sucrose laurate ester; EggPC, egg phosphatidylcholine; Chol, cholesterol; CS, cholesterol sulfate; TEM, cryo-transmission electron microscopy; FFEM, freeze-fracture electron microscopy; TPE, Two-photon fluorescence microscopy

* Corresponding author. Fax: +31-71-527-4565.

0005-2736/99/$ – see front matter
PII: S0005-2736(99)00176-5

riched intercellular matrix. The permeability barrier is located within the lipid lamellae in the intercellular spaces of the stratum corneum [1–7]. The lipid lamellae are formed by rearrangement of lamellar disks that are extruded from the uppermost cells of the stratum granulosum [4].

To broaden the spectrum of drugs delivered via the skin and to increase efficacy of systemic treatment, there is a demand for new transdermal drug delivery systems. Vesicles have been developed as possible carriers in transdermal drug targeting by facilitating the transdermal drug transport through specific interactions with skin. It has been suggested that skin–vesicle interactions are influenced by both, chemical characteristics of vesicles, e.g. their composition and charge, and physical, such as physical state, lamellarity, and size [8–12]. In addition, interactions are also influenced by the application method, such as occlusive or non-occlusive application [13], and general skin conditions.

There is still debate concerning the mechanisms by which vesicles facilitate (trans)dermal diffusion of drugs. So far, three main mechanisms have been described by which vesicles interact with the stratum corneum: (1) penetration of intact vesicles into the stratum corneum where the vesicles either localize [14] or pass on to the dermis [15]; (2) adsorption or fusion of vesicles on the surface of the skin [10,16]; and (3) penetration of vesicle constituents into the skin which may affect the ultrastructure of the intercellular regions in the stratum corneum [17,18].

Most of the research involving both the investigation of mechanisms by which vesicles interact with skin as well as their use as drug carriers for transdermal drug delivery has focussed on vesicles composed of phospholipids (liposomes) or non-ionic surfactants (niosomes). Fluidization of intercellular domains and thus a structural modification of the stratum corneum has been suggested as a possible mechanism for the enhanced drug transport of encapsulated drugs in vesicles. Stratum corneum may also act as a reservoir for topically applied substances [19] and can be studied to elucidate the mechanism involved in (trans)dermal transport [20]. Techniques to penetration pathways of either vesicle constituents or (model) drugs are confocal laser scanning microscopy (CLSM) [6,21] or two-photon excitation microscopy (TPE). Techniques to study the mechanisms involved in vesicle–skin interactions are transmission electron microscopy (TEM) [16,22], freeze-fracture electron microscopy (FFEM) [6,10, 23], X-ray diffraction and electron spin resonance (ESR) [9,17].

On the basis of physicochemical considerations, Cevc [24] developed elastic vesicles, named Transfersomes, to enhance drug transport through the stratum corneum into the viable epidermis. They postulated that penetration of intact vesicles into the stratum corneum and underlying tissue is possible under certain conditions, i.e. non-occlusive application of elastic vesicles [25]. The hydration driving force for these specific elastic vesicles into the skin is larger than the resistance when passing intercellular lipid regions in the stratum corneum. The driving force is generated by a large hydration gradient across the skin, varying from 15 to 20% in the stratum corneum to 70% in the stratum granulosum.

The objective of this study was to elucidate possible mechanisms by which elastic liquid-state vesicles may interact with human skin and hence contribute to transdermal drug delivery. Since the physicochemical characteristics of vesicles influence interactions with skin, a number of liquid-state vesicle formulations with varying compositions were investigated.

By combining surfactants, which by themselves form bilayers, with micelle forming single-chain surfactants, vesicles can be developed with varying elasticities depending on the molar ratio of the components. It is the simultaneous presence in one membrane of different stabilizing/destabilizing molecules, and their tendency to redistribute in the bilayers that enables these vesicles to be more elastic compared to conventional liposomes and niosomes [24].

In our studies elastic vesicles were based on the single-chain non-ionic surfactant octaoxyethylenelaurate-ester (PEG-8-L) combined with either egg phosphatidylcholine (EggPC) (unsaturated C18-chain) or sucrose-ester L-595 (saturated C12-chain), with and without cholesterol sulfate, whereas rigid vesicles were composed of either the sucrose-ester L-595 or Wasag-7 (C18), cholesterol and cholesterol sulfate. In

previous studies, we investigated the stability, morphology and elasticity of these vesicle formulations [26]. The vesicles were considered to be elastic when it was possible to extrude the formulations through membranes with 30-nm pores.

In the present study, TEM in combination with ruthenium tetroxide (RuO_4) and FFEM has been used to visualize interactions of elastic vesicles and rigid vesicles with human skin at an ultrastructural level. In addition to TEM and FFEM, TPE was used to study interactions and penetration pathways of vesicle constituents. TPE is a sensitive technique for the 3D-imaging of skin on a light microscopic level. When using conventional (single-photon) confocal fluorescence microscopy, the scattering of the emitted fluorescence light is a major problem in the visual sectioning of fluorescence as a function of skin depth. By using a longer wavelength, TPE reduces this scattering and the penetration depth is therefore increased. Furthermore, in single-photon imaging, bleaching occurs over the whole illumination cone while in TPE, photobleaching is confined to the focal volume. When scans are made at different axial positions bleaching in two-photon microscopy is reduced considerably and makes TPE the preferred tool for direct visualization of diffusion of fluorescent molecules through skin.

2. Materials and methods

2.1. Materials

The sucrose-ester Wasag-7 was purchased from Schmidt (Amsterdam, The Netherlands), whereas the sucrose laurate-ester L-595 was a gift from Mitsubishi Kasei (Tokyo, Japan). Wasag-7 consists of 70% stearate-ester and 30% palmitate-ester (40% mono, 60% di/tri-ester) (HLB = 7); L-595 consists of 100% laurate-ester (30% mono-, 40% di-, 30% tri-ester) (HLB = 7). The polyoxyethylene laurate ester PEG-8-L was a gift from Lipo Chemicals (Paterson, NJ, USA). Cholesterol (Chol) and cholesterol sulfate (CS) were purchased from Sigma (Hilversum, The Netherlands). Egg phosphatidylcholine (EggPC) was obtained from Avanti Polar Lipids (Pelham, AL, USA). The buffer used was a phosphate buffered saline (PBS) pH 7.4 (8 mM Na_2HPO_4, 1.5 mM KH_2PO_4, 139 mM NaCl, 2.5 mM KCl in millipore water). Fluorescein-DHPE was purchased from Molecular Probes (Eugene, OR, USA).

Table 1
Composition of vesicle formulations in molar ratio

Formulations	Composition (mol%)
1. PEG-8-L:L-595	30:70
2. PEG-8-L:L-595	70:30
3. PEG-8-L:L-595:CS	30:70:5
4. PEG-8-L:L-595:CS	70:30:5
5. PEG-8-L:EggPC	30:70
6. PEG-8-L:EggPC	70:30
7. Wasag-7:Chol:CS	50:50:5
8. L-595:Chol:CS	50:50:5

PEG-8-L, octaoxyethylenelaurate-ester; L-595, sucrose laurate ester, EggPC, egg phosphatidylcholine; Chol, cholesterol, CS, cholesterol sulfate.

2.2. Preparation of vesicle formulations

The composition and molar ratio of vesicle formulations is shown in Table 1. Vesicles were prepared by a modification of the sonication method described by Baillie et al. [27]. The surfactants, cholesterol and cholesterol sulfate were solubilized in chloroform/methanol (3:1 v/v). Subsequently, the solvent was evaporated by leading a N_2-stream in tubes containing the solvent at 40°C and the remaining surfactant film was hydrated with PBS pH 7.4. The final formulation contained 5% (w/w) of lipids.

Vesicle formulations composed of PEG-8-L:L-595:CS and PEG-8-L:EggPC were sonicated for 15 s at room temperature, whereas vesicles composed of Wasag-7 and L-595 in combination with cholesterol and cholesterol sulfate were heated to 80°C to dissolve the lipid film and sonicated for 45 s. The sonicator used was a Branson Sonifier 250 (Branson Ultrasonics, Danbury, CT) with an 1/8 in. microtip at 60 Watt energy output.

The formulations were cooled down to room temperature and examined for phase separation, vesicle formation and crystal formation using a polarization microscope. The vesicle diameter was between 100 and 150 nm as determined by dynamic light scattering.

2.3. Skin preparation

Human abdominal skin was obtained after cosmetic surgery and processed the same day. Subcutaneous fat was removed and skin dermatomed to a thickness of approximately 200–250 μm (Padgett Dermatome, Kansas City, USA).

2.4. Transmission electron microscopy and freeze-fracture electron microscopy

Circular pieces of skin (∅ 18 mm) were placed in Franz-type diffusion cells with the stratum corneum side facing the donor compartment. The receiver compartment was filled with PBS pH 7.4 and heated to 37°C to establish a temperature of 32°C on the skin surface. Care was taken to prevent the occurrence of air bubbles between the dermal side of skin and receiver solution. Following the mounting of the skin, 50 μl/cm^2 of vesicle formulation was applied to the stratum corneum and carefully spread to achieve complete and homogeneous surface covering. A minimum of two cells using skin from at least two different donors was used. All experiments were carried out under non-occlusive conditions for a period of 16 h.

Skin samples were removed immediately following the 16-h application period and biopsies were taken both for TEM and FFEM. For TEM, biopsies (1×4 mm) were fixed at 4°C in Karnovsky's fixative overnight and with a combination of osmium tetroxide and ruthenium tetroxide +0.25% (w/v) $K_3Fe(CN)_6$ [28]. Following fixation, the samples were dehydrated in a range of ethanol solutions (70, 90, 95, 100%) and embedded in Spurr's resin. Ultrathin sections were cut (Ultracut E, Reichert-Jung, Vienna, Austria), collected on formvar coated grids and examined in a Philips 410 (Philips, Eindhoven, The Netherlands) electron microscope. Approximately five overview and 30–40 detailed micrographs were taken of each treatment and compared with PBS-treated skin.

For FFEM, skin samples were processed as described elsewhere [29]. After the freeze-fracture procedure, the replicas were cleaned in 0.5 M ammonium hydroxide in Toluene (Soluene-350, Packard Instrument Company, Meriden, USA) for 5 days. After Soluene treatment, Soluene was removed by washing the replicas with toluene. The replicas were collected on 400 mesh copper grids (Balzers, Liechtenstein) and examined in a Philips EM410 (Philips, Eindhoven, The Netherlands) transmission electron microscope operated at 80 kV. For each treatment, 30–40 micrographs were taken and evaluated.

2.5. Two-photon excitation microscopy

TPE was used to visualize the effect of treatment with vesicles on the penetration of a fluorescence label into skin. To visualize the skin structure and morphology, untreated skin was stained for 16 h by submerging the skin in either a fluorescein solution in the absence of vesicles.

Skin treated with PEG-8-L:L-595:CS (70:30:5) vesicles, Wasag-7:Chol:CS (50:50:5) vesicles and PEG-8-L micelles was investigated. For vesicles and micelles, the fluorescence label fluorescein-DHPE was incorporated at a molar ratio of 2.75% during the preparation procedure. In total, three skin samples (∅ 18 mm) of at least three different donors per vesicle formulation and application period were clamped between donor and receiver compartment of Franz-type diffusion cells under the same conditions as described above for TEM and FFEM visualization experiments. Vesicle formulation (50 μl/cm^2) was administered non-occlusively for 1, 3, 6 and 16 h, after which, skin samples were removed, washed and sandwiched in between two microscope coverslips without intermediate fluid for imaging. Two-photon fluorescence microscopic images were recorded with the set-up as described by Vroom [30]. *xy*-Images comprising 256×256 pixels (16 bits) were recorded at different axial positions in skin. The field of view of these images was 110×110 μm^2 and the pixel dwell time was 128 μs. The average power on the sample was approximately 5 mW. The refractive index of the stratum corneum was about 1.55 [31], close to that of immersion oil ($n_D \sim 1.515$). A 60×NA 1.4 oil-immersion objective (Nikon, Japan) was therefore used for the imaging of vesicle transport pathways through skin. The excitation wavelength was 800 nm and leaked stray excitation light in the detection path was blocked by a series of 700 nm short-pass interference filters (Optosigma) and placed in front of the photomultiplier. In obtaining the images, the same settings of the microscope were always used.

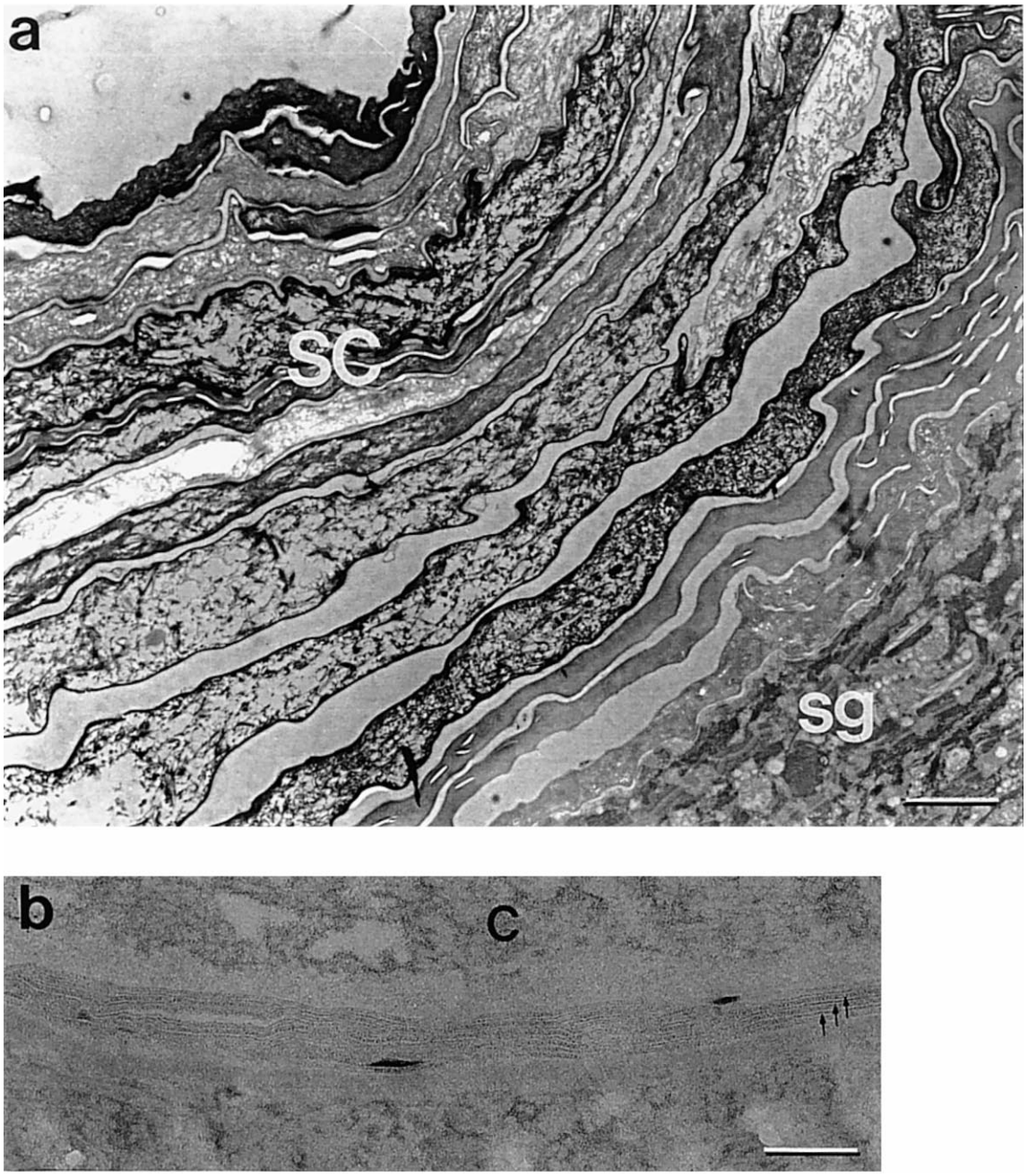

Fig. 1. TEM micrographs of human skin incubated non-occlusively with PBS for 16 h. (a) Overview stratum corneum (sc) and the upper part of the stratum granulosum (sg). Scale bar: 2 μm. (b) Detailed electron micrograph of the stratum corneum showing intercellular lipids (arrows), and keratin-filled corneocytes (C). Scale bar: 100 nm.

3. Results

3.1. Transmission electron microscopy

In Fig. 1, representative electron micrographs of PBS-treated skin are shown. The RuO_4-fixation is limited to a maximum of six to eight cell layers from the skin surface downwards. Therefore, lamellae in lower parts of the stratum corneum cannot be visualized and consequently intercellular spaces appear as 'empty'. The micrographs in Fig. 1 clearly show corneocytes, flattened cells characterized by

the absence of cell organelles and the presence of electron dense keratin filaments. In intercellular spaces, lipid lamellae are visualized, whereas sebaceous lipids, observed as smooth gray areas, are present on the surface of the stratum corneum and between upper stratum corneum cell layers. Below the stratum corneum, the stratum granulosum can be identified.

Elastic liquid-state vesicles (Fig. 2) appear on the surface of the skin as aggregates filled with lipid material. In Fig. 2a, an overview of skin treated with PEG-8-L:EggPC (30:70) vesicles is presented. This particular area contains a skin wrinkle in which vesicles close to the skin surface have not been washed away during the fixation procedure. Vesicle material within the intercellular spaces of the upper three to four corneocytes of the stratum corneum is observed as either: (1) spherical lipid aggregates surrounded by electron dense material; (2) lipid aggregates containing small electron dense spots; or (3) small oligolamellar spherical structures. Occasionally, in the upper 2–3 cell layers, small intracellular lipid aggregates were observed, whereas lipid aggregates fused onto the corneocyte envelope (Fig. 2b).

Treatment of skin with 30:70 and 70:30 PEG-8-L:L-595 vesicle formulations induced ultrastructural changes similarly as observed for PEG-8-L:EggPC vesicles. However, in one donor treated with PEG-8-L:L-595 (70:30) vesicles, large areas of bilayer stacks were observed different in appearance than stratum corneum lipid lamellae and were present throughout the entire stratum corneum. In some regions, it was observed that these lamellar stacks disorganized intercellular stratum corneum lipid lamellar stacking (Fig. 3) by pushing them apart. The bilayers in these stacks were occasionally orientated perpendicular to the stacking of the stratum corneum lamellae (Fig. 3c) or when accumulated, they were orientated randomly (Fig. 3d).

The addition of CS to PEG-8-L:L-595 did not have an additional effect on the interactions or penetration depth of vesicle material; the same ultrastructural changes were observed as in skin treated with PEG-8-L:L-595 vesicles without CS. Fig. 3e shows a representative example of skin treated with PEG-8-L:L-595:CS (30:70:5) vesicles. After treatment with PEG-8-L:L-595:CS (70:30:5) vesicle formulations similar structures were found (not shown).

After treatment with PEG-8-L-containing vesicle formulations, areas of lipids with electron dense material have been visualized deeper down in the stratum corneum that is fixed only by OsO_4. Since SC lipid lamellae cannot be fixed by OsO_4 [28], the lipid material has to be originated from the vesicles. These OsO_4 fixed lipid areas, containing electron dense material (see for example Fig. 3e), have not been observed in PBS-treated skin. No ultrastructural changes were observed in cell layers below the stratum granulosum (not shown).

Treatment of skin with L-595:Chol:CS (50:50:5) vesicles revealed the presence of vesicle material on the surface of skin, most likely mixed with sebaceous lipids (not shown). Lipid material with electron dense spots similar to those observed after treatment with elastic liquid–state vesicles were only observed between the upper 2–3 cell layers and not deeper down in the stratum corneum. Wasag-7:Chol:CS (50:50:5) vesicles (Fig. 4) induce no ultrastructural changes in the stratum corneum.

3.2. Freeze-fracture electron microscopy

Fig. 5a and b show representative electron micrographs of PBS-treated skin. Keratin filaments are shown as particles that entirely fill the interior space of corneocytes, whereas cell organelles are absent. Mostly, the fracture plane in the corneocyte is orientated perpendicular to the skin surface. In intercellu-

→

Fig. 2. TEM micrographs of human skin incubated non-occlusively with PEG-8-L:EggPC (30:70) vesicles for 16 h. (a) An overview electron micrograph of skin treated with PEG-8-L:EggPC (30:70) vesicles. This area contains a skin wrinkle in which vesicles close to the skin surface have not been washed away during the fixation procedure. Vesicles appear on the skin surface as droplets (aggregates) filled with lipid material. Scale bar: 5 μm. (b) Material originating from vesicles (V) is present within intercellular spaces of the upper three to four corneocytes and appear as aggregates surrounded by electron dense material (arrows) and small lipid droplets are observed intracellularly (arrowheads) which fuse onto the corneocyte envelope. Scale bar: 0.5 μm. C, corneocyte; SG, stratum granulosum; SC, stratum corneum; asterisk, vesicles; V, material originating from vesicles.

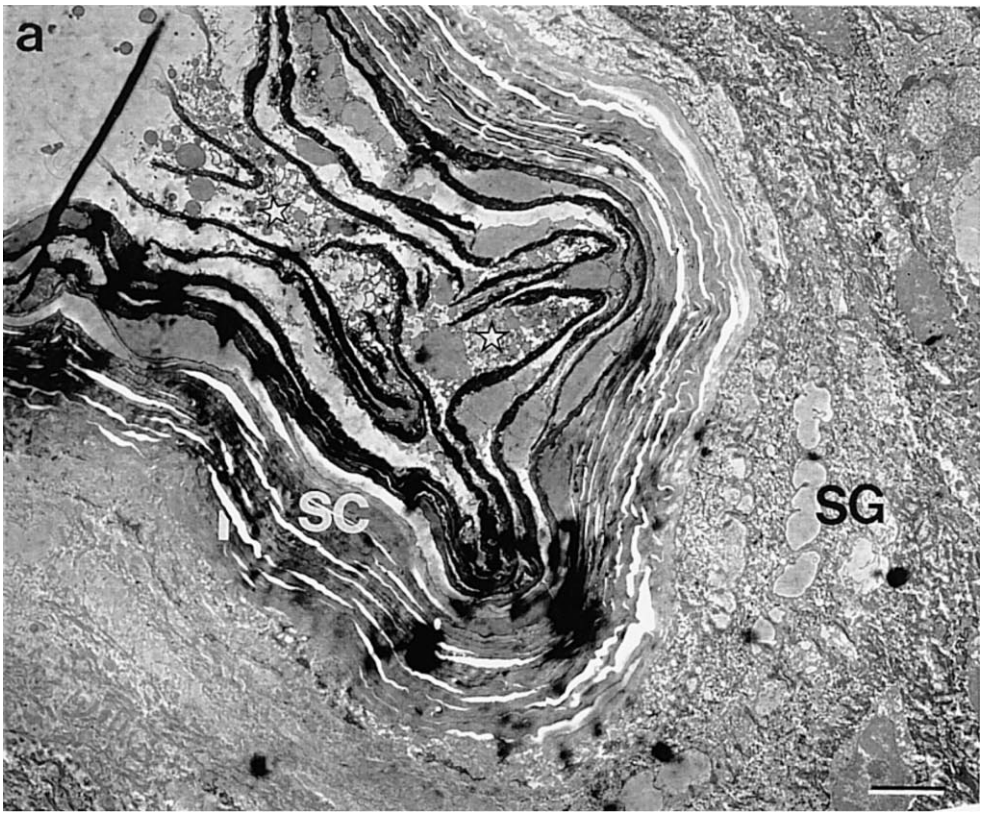
a
SC
SG

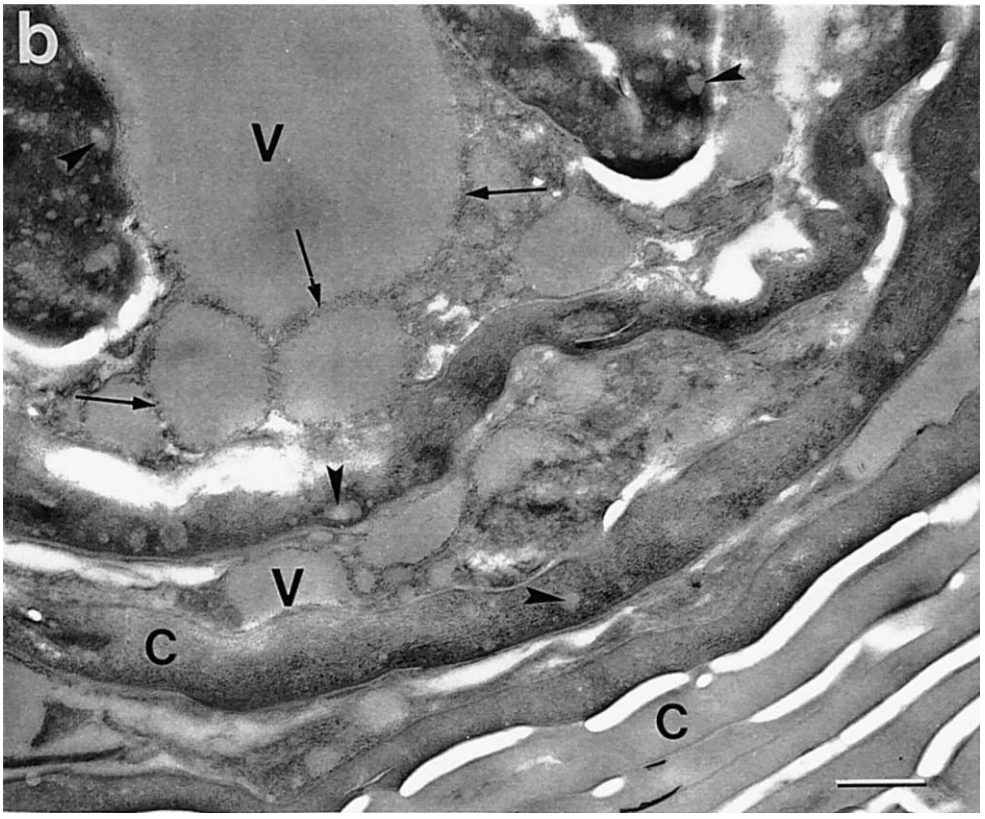
b
V
V
C
C

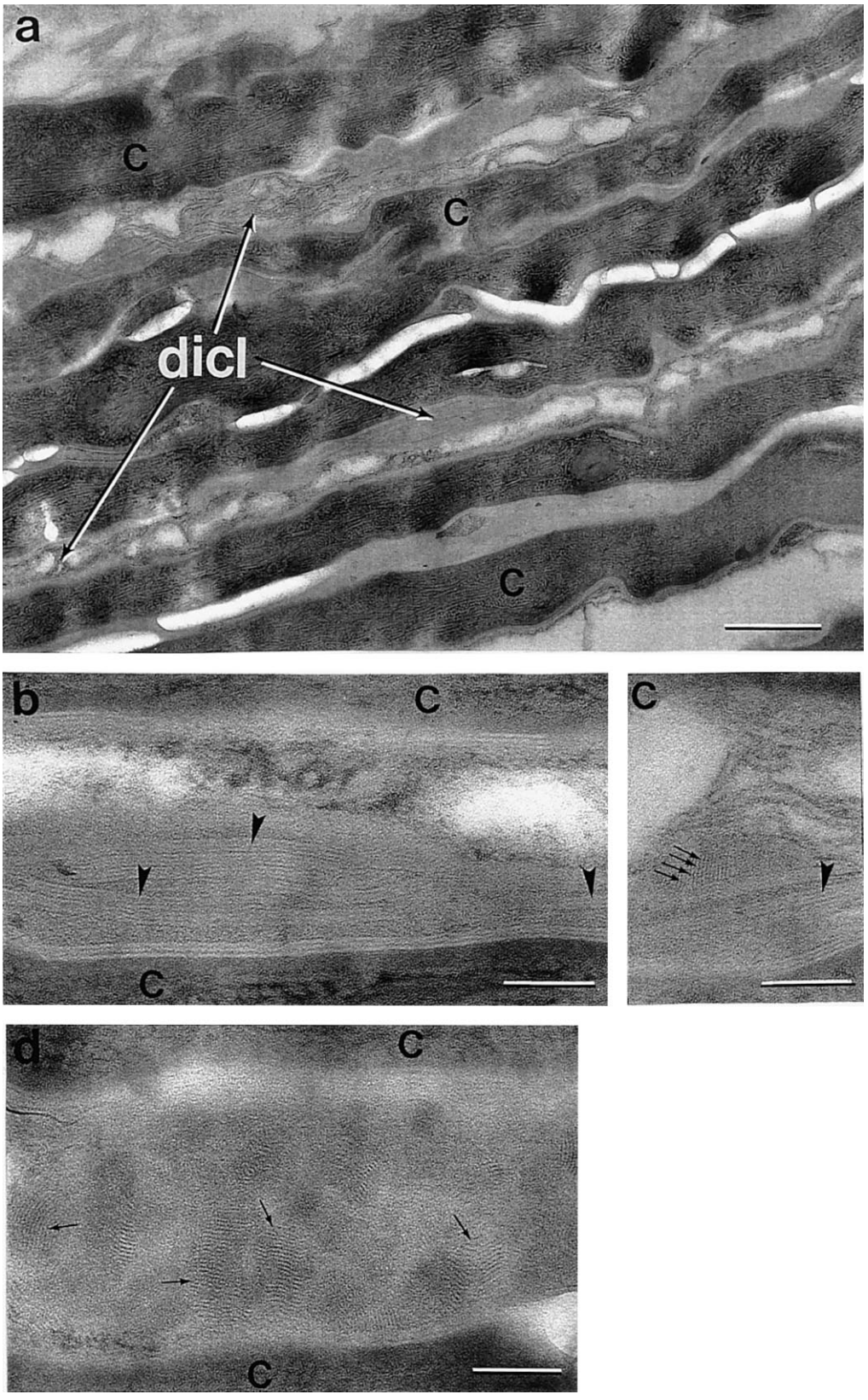
a
C
C
dicl
C
b
C
C
c
d
C
C

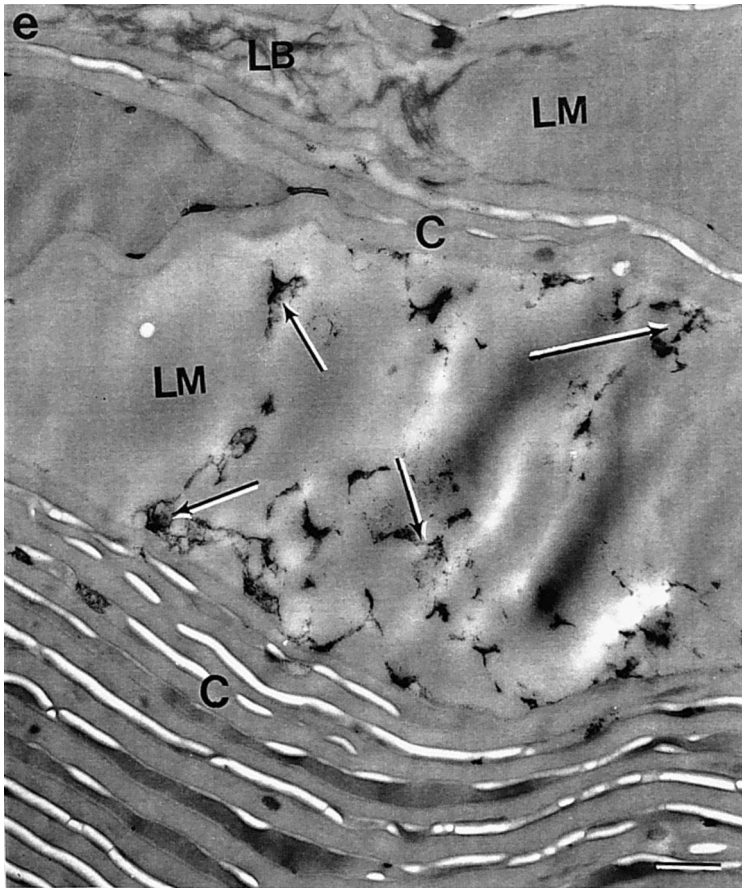

Fig. 3. TEM micrographs of human skin incubated non-occlusively with PEG-8-L:L-595 vesicles (70:30) for 16 h. (a) Overview of stratum corneum with disorganized intercellular lipids (dicl). Scale bar: 200 nm. (b) A detailed micrograph of disorganized intercellular lipid bilayers. Bilayers appear to be detached from each other in units of three bilayers (arrowheads). Scale bar: 100 nm. (c) Frequently, stacks of bilayers which resemble stacked flattened vesicles, were observed with its bilayers oriented perpendicular to skin lipid bilayers and cell membranes (arrows); arrowhead, unit of three skin lipid bilayers. Scale bar: 100 nm. (d) Detailed micrographs of intercellular spaces filled with round and oval stacks of bilayers (arrows) oriented at random. Scale bar: 100 nm. (e) TEM micrographs of human skin incubated non-occlusively with PEG-8-L:L-595:CS vesicles (70:30:5) for 16 h. Electron micrograph of osmium fixed stratum corneum at a depth of approximately 10 μm. Extensive lipid areas (LM) with electron dense material (arrows) and lipid bilayers (LB) are fixed by osmium tetroxide. Scale bar: 500 nm. C, corneocyte.

lar spaces, however, the fracture plane goes along the lamellae of multi-layered arranged lipids. The intercellular lipid lamellar regions are presented as smooth surface planes resulting from fractures along lamellae. When the fracture plane crosses lipid lamellae, sharp edges appear. Desmosomes are observed in intercellular spaces as areas with aggregated particles and are observed throughout the stratum corneum.

After incubation of skin with liquid-state vesicles containing PEG-8-L and L-595, a very distinctive effect on the ultrastructure of intercellular lipid lamellae was observed. Fig. 6 demonstrates skin treated with PEG-8-L:L-595:CS (70:30:5). Large intercellular lipid areas are observed and have an irregular appearance. The large lipid fracture planes through intercellular spaces are caused by a decrease in resistance within these areas indicating a reduced cohesive force between the lipid lamellae. Distinctive desmosomes are less frequently observed compared to PBS-treated skin and edges that are a result of cross fracturing the lipid lamellae are less sharp. The decrease in desmosome density in the fracture planes is most probably caused by another route of the fracture through the SC. Since the fracture plane is located in regions of least resistance, it most probably chooses the regions containing a high content of

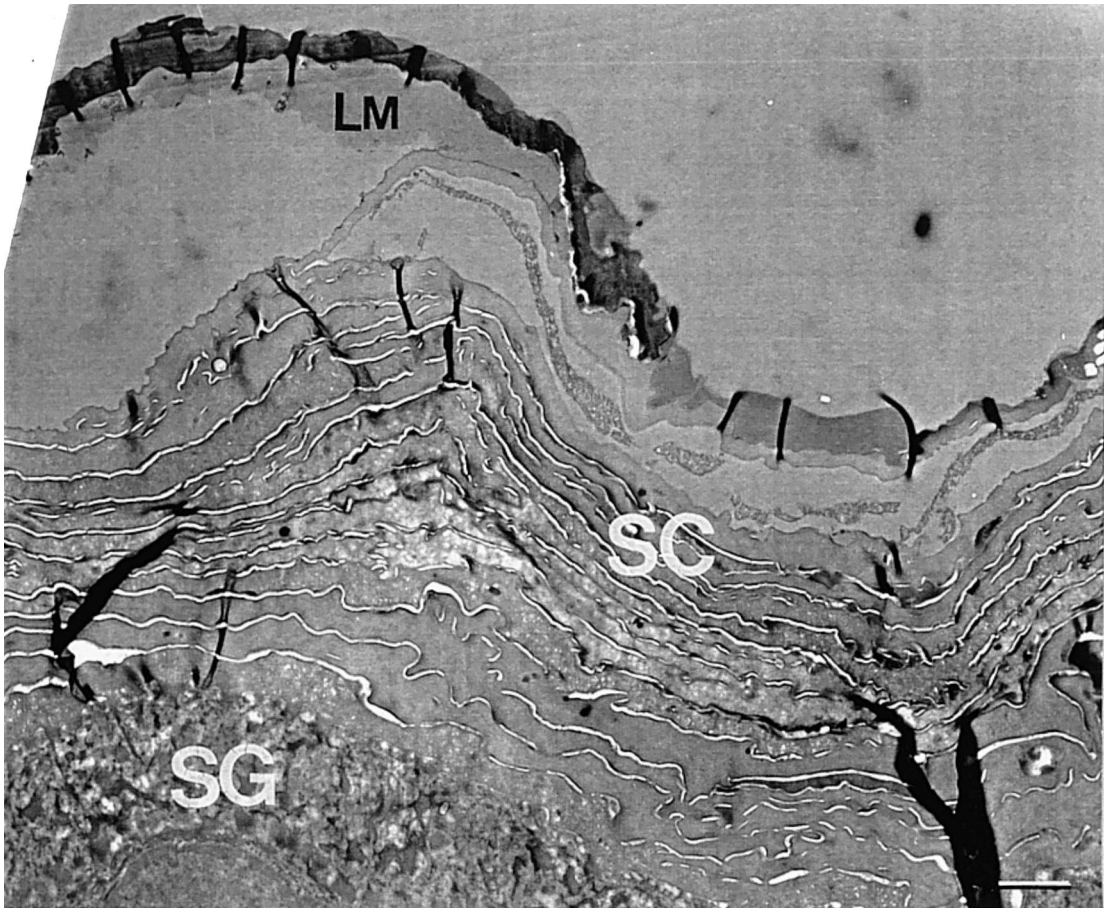

Fig. 4. Overview of stratum corneum (SC) of skin treated with Wasag-7 vesicles with lipid material (LM) present in between upper two cell layers. Scale bar: 10 μm. SG, stratum granulosum.

lipids/surfactants (from the vesicles). Large intercellular lipid areas are also present in skin treated with PEG-8-L:EggPC (30:70) vesicles (not shown). Interfacial interactions, such as vesicle adsorption or fusion were not visualized in skin treated with any of the elastic liquid-state vesicle formulations.

Treating skin with both cholesterol containing vesicle formulations did not change the ultrastructure of stratum corneum. No differences were found between skin treated non-occlusively for 16 h with Wasag-7 or L-595 vesicles. Desmosomes were clearly visualized in intercellular spaces between corneocytes, whereas lipid bilayers appeared smooth (not shown). Again, vesicle adsorption or fusion at the vesicle-skin interface was not visualized.

3.3. Two-photon excitation microscopy

Fig. 7 illustrates the skin structure and morphology of skin after staining by submersion for 16 hours in fluorescein in the absence of vesicles. In Fig. 7a and b, an *xz*-image and *xy*-image (95×95 μm^2) are shown, respectively, of fluorescein stained skin. Parallel to the skin surface, a white (high intensity) area

→

Fig. 5. Freeze-fracture electron micrographs of human abdominal skin treated non-occlusively with PBS for 16 h. (a) Corneocytes (C) are shown, which can be recognized by their granular appearance resulting from keratin filaments. Scale bar: 500 nm. (b) High magnification micrograph of the intercellular space between two adjacent corneocytes (C). Desmosomes (D) are visualized as aggregated particles. The intercellular lipid matrix (icl) is organized in lipid lamellae (arrows) and when fractured can appear as steps (arrows).

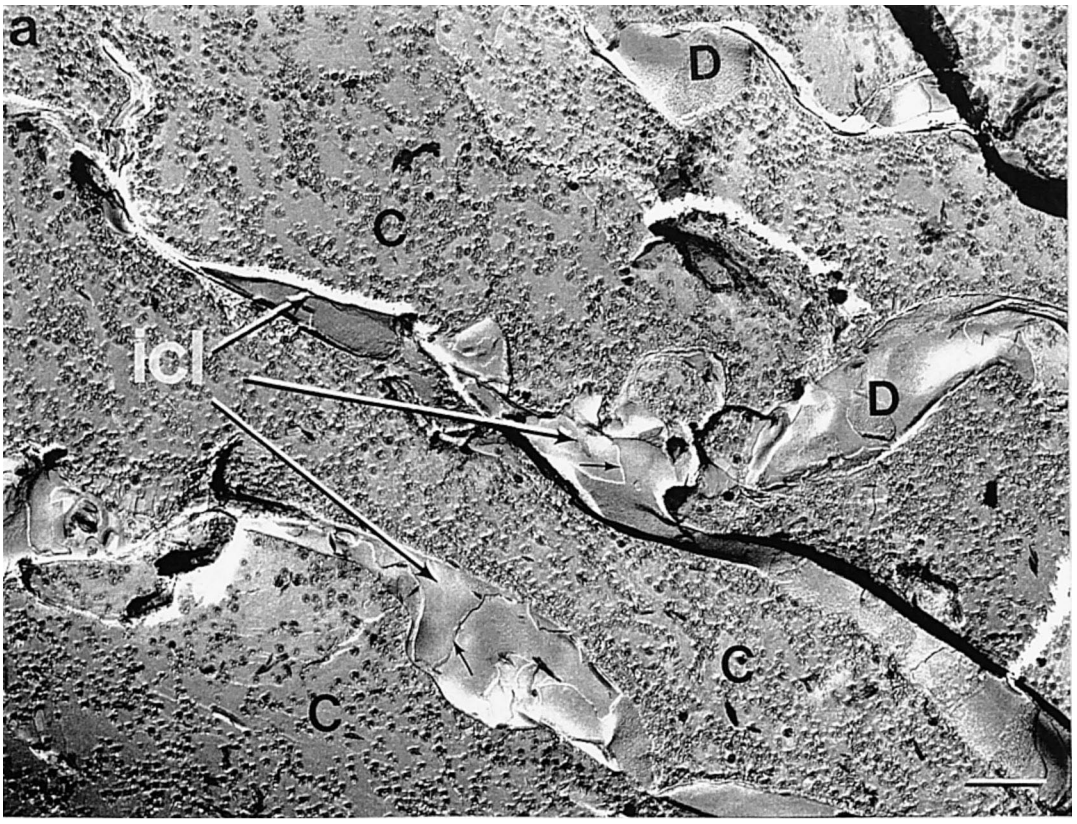
a
D
C
icl
D
C
C

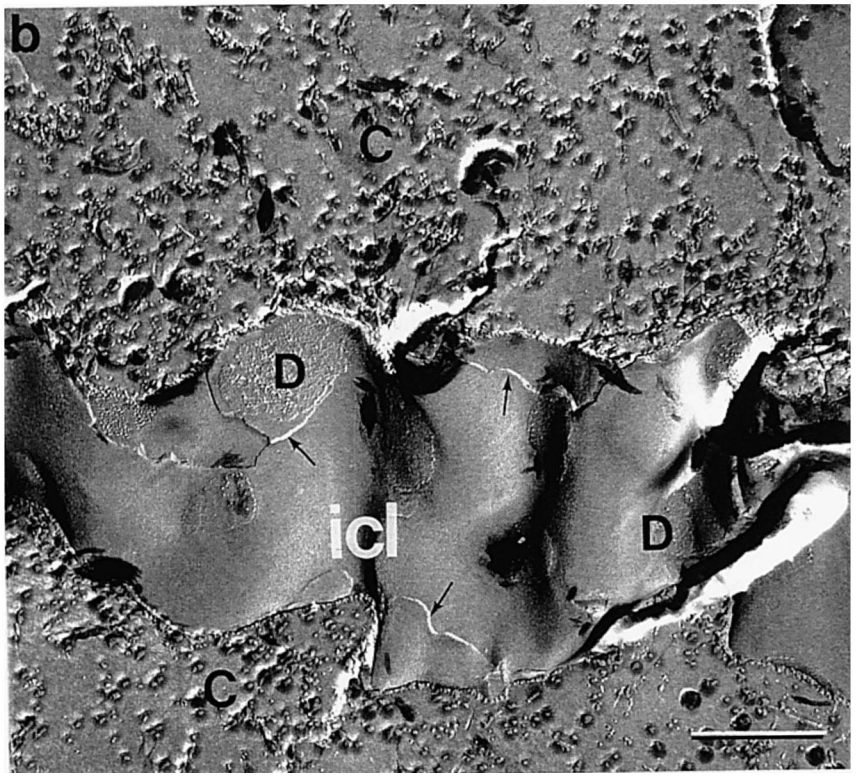
b
C
D
icl
D
C

appears at the surface of the skin which corresponds to fluorescence from dissolved dye in the buffer (Fig. 7a). Stratum corneum itself is observed as a dark band, which indicates that fluorescein has not penetrated into intercellular spaces between corneocytes to stain the highly impermeable lipid bilayers. Below the stratum corneum, various layers of the epidermis are visualized in which fluorescein mainly stains cell membranes. After applying vesicle formulations for several periods varying between 1 and 16 h, penetration pathways of vesicle constituents in the stratum corneum were studied by recording *xy*-images at different depths in skin samples.

Fig. 8a illustrates an *xy*-image (95×95 μm^2) recorded at a depth of 10 μm in skin treated with PEG-8-L:L-595:CS (70:30:5) elastic vesicles. Already after 1 h of application, a fine meshwork of 'channels' was observed without any distinguishable polygonal cell contours. The distance between these channels was approximately 5 μm. The channels appear immediately after drying of the liquid-state vesicle formulation. There was no relationship between application period and depth at which fluorescence was detected.

In Fig. 8b an *xy*-image (95×95 μm^2) is shown, recorded at a depth of 3 μm into the stratum corneum treated with rigid Wasag-7 vesicles. The polygonal shape of corneocytes can clearly be distinguished and indicates a rather homogeneous intercellular penetration of fluorescence label. It is important to stress that the thickness of corneocytes is 0.5–1 μm, which is in the order of the axial size of the focal spot. The stack of lipid lamellae surrounding each corneocyte has a thickness of approximately 50–100 nm, which is below the axial resolution. If fluorescent material is distributed homogeneously between intercellular lipid lamellae, fluorescence in vertical cell borders will contribute several times higher to the measured intensity than fluorescence in horizontal lamellae and therefore cell borders appear bright. No contribution from fluorescence in the interior of corneocytes was observed. The total penetration depth of the Wasag-7 vesicle constituents was only a few microns. Fig. 9 shows *xy*-images at different depths of skin treated with elastic liquid-state vesicles. Again, thread-like channels are formed in the entire stratum corneum. However, no fluorescence was detected further down into the stratum granulosum or stratum spinosum. When no additional staining is used (not shown) only black areas are found in the regions below the stratum corneum. However, by staining with acridine orange for 1 h subsequently to the vesicle treatment, the stratum granulosum is visualized and provides an indication of the location of the interface with the stratum corneum. Fig. 10 illustrates *xy*-images at several depths in skin treated with micelles composed of 100 mol% PEG-8-L. The polygonal shape of corneocytes is clearly visualized and fluorescence was detected to a depth of approximately 3 μm in the stratum corneum.

4. Discussion

The objective of this study was to investigate the effects of elastic and rigid vesicle formulations on human skin, in vitro, in relation to their composition. These elastic vesicle formulations are intended to be used for topical drug application of amphiphilic or lipophilic drugs and their composition may be optimized to improve dermal or transdermal drug delivery. The combination of the visualization techniques TEM, FFEM and TPE was chosen to study structure modulation and penetration pathways of vesicle constituents in detail. In earlier studies, extensive characterization of both skin [28] and vesicles formulations [26] have been performed. Vesicles prepared by sonication consist of uni- or oligolamellar bilayers. Electron spin resonance and extrusion measurements revealed that vesicles containing the surfactant PEG-8-L consist of elastic bilayers [26]. Increasing the amount of PEG-8-L in bilayers increased the elasticity, which could be fa-

→

Fig. 6. Freeze-fracture electron micrographs of human abdominal skin treated non-occlusively with liquid-state PEG-8-L:L-595:CS (70:30:5) vesicles for 16 h. (a) Large intercellular lipid areas (icl) were observed with an irregular appearance. Scale bar: 2 μm. (b) High magnification micrograph of irregular intercellular lipid regions. Distinctive desmosomes are absent. Granular regions are present (arrowheads). The edges from lamellar steps are less sharp than in PBS-treated skin (arrows). Scale bar: 500 nm. C, corneocyte.

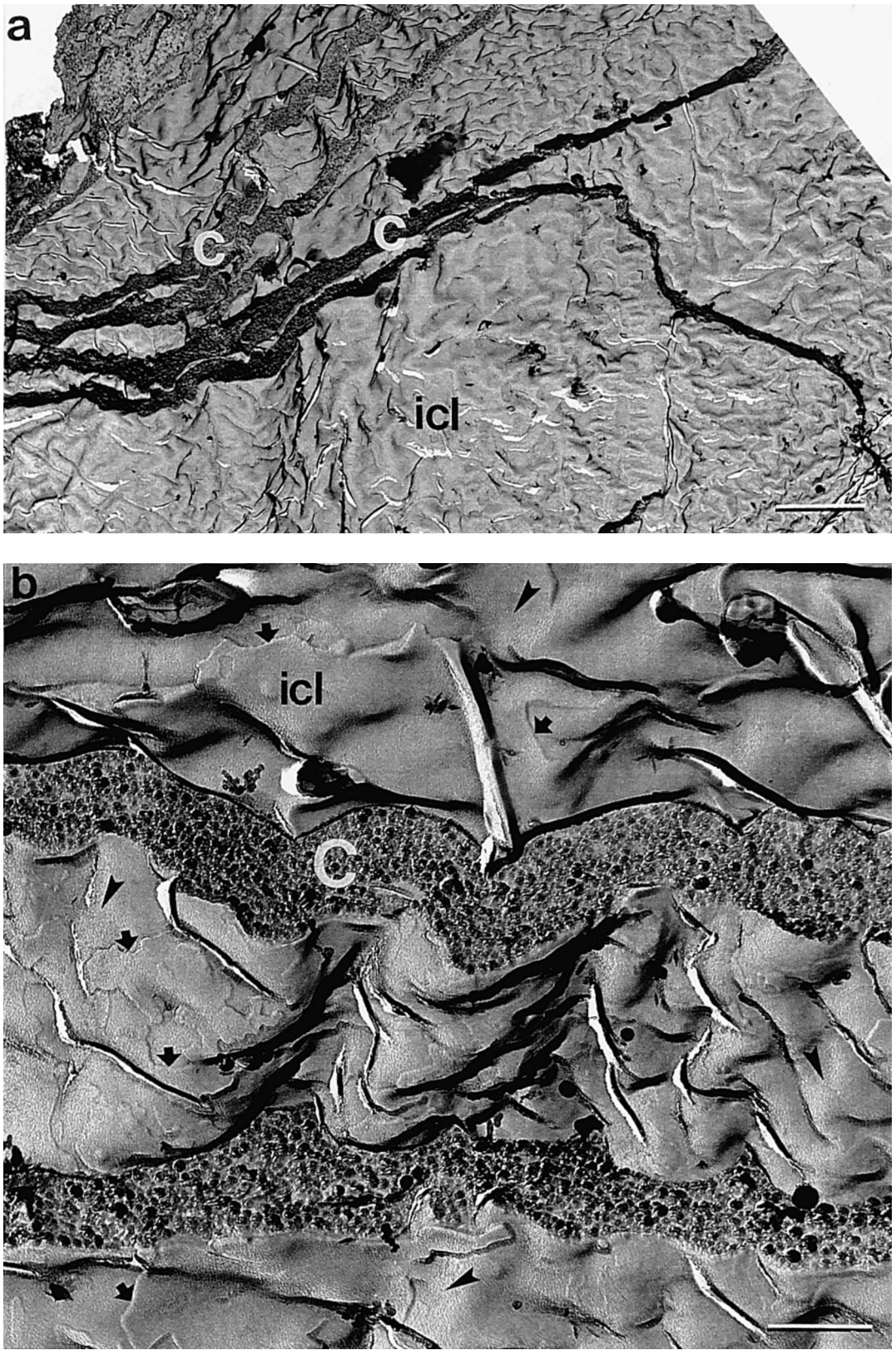
a
c
c
icl
b
icl
c

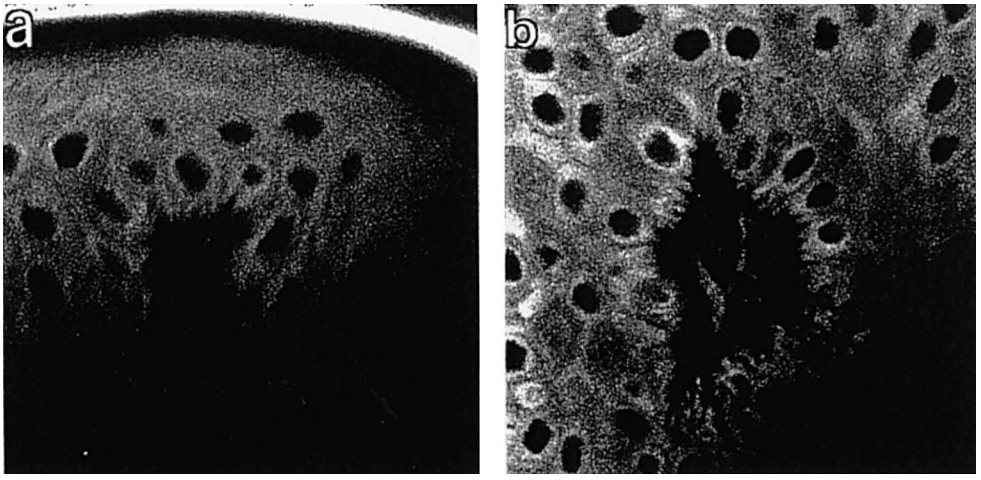

Fig. 7. TPE of skin stained with fluorescein. (a) *xz*-Image (95×95 μm^2). Parallel to the skin surface, a white (high intensity) area appears at the skin surface, which corresponds to fluorescence from dissolved dye in the buffer. In the dark band below, the stratum corneum is located. (b) *xy*-Image (95×95 μm^2) at a depth of 150 μm, revealing the stratum basale and stratum spinosum.

vorable for topical application. On the other hand, when the unilamellar bilayers become saturated with PEG-8-L, perforated bilayers in combination with thread-like micelles were formed which destabilize vesicles. Therefore, an optimum in elasticity and stability of vesicles is crucial for their use in dermal or transdermal drug delivery. In this study, we examined the relationship between the elasticity and composition of vesicles and their interactions with human skin, in vitro.

4.1. Transmission electron microscopy

Upon in vitro application of vesicle formulations

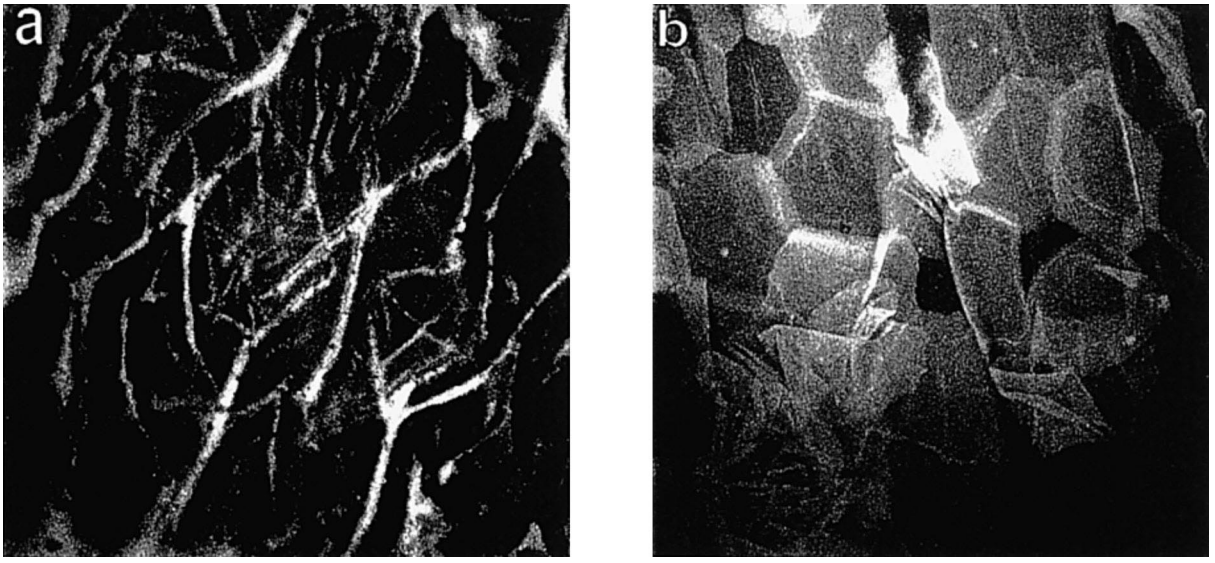

Fig. 8. TPE images of skin treated with PEG-8-L:L-595:CS (70:30:5) vesicles (a). *xy*-Image (95×95 μm^2) recorded at a depth of 10 μm in skin treated with PEG-8-L:L-595:CS (70:30:5) liquid-state vesicles. After 1 h of application, already a fine meshwork of 'channels' was observed without any distinguishable polygonal cell contours. The distance between these channels was approximately 5 μm. Channels appear immediately after drying of the liquid-state vesicle formulation. TPE images of skin treated with rigid Wasag-7 vesicles. (b) *xy*-Image (95×95 μm^2) recorded at a depth of 3 μm in stratum corneum The contours of the polygonal shaped cells are clearly depicted in contrast to image of the stratum corneum obtained after treatment with elastic vesicles.

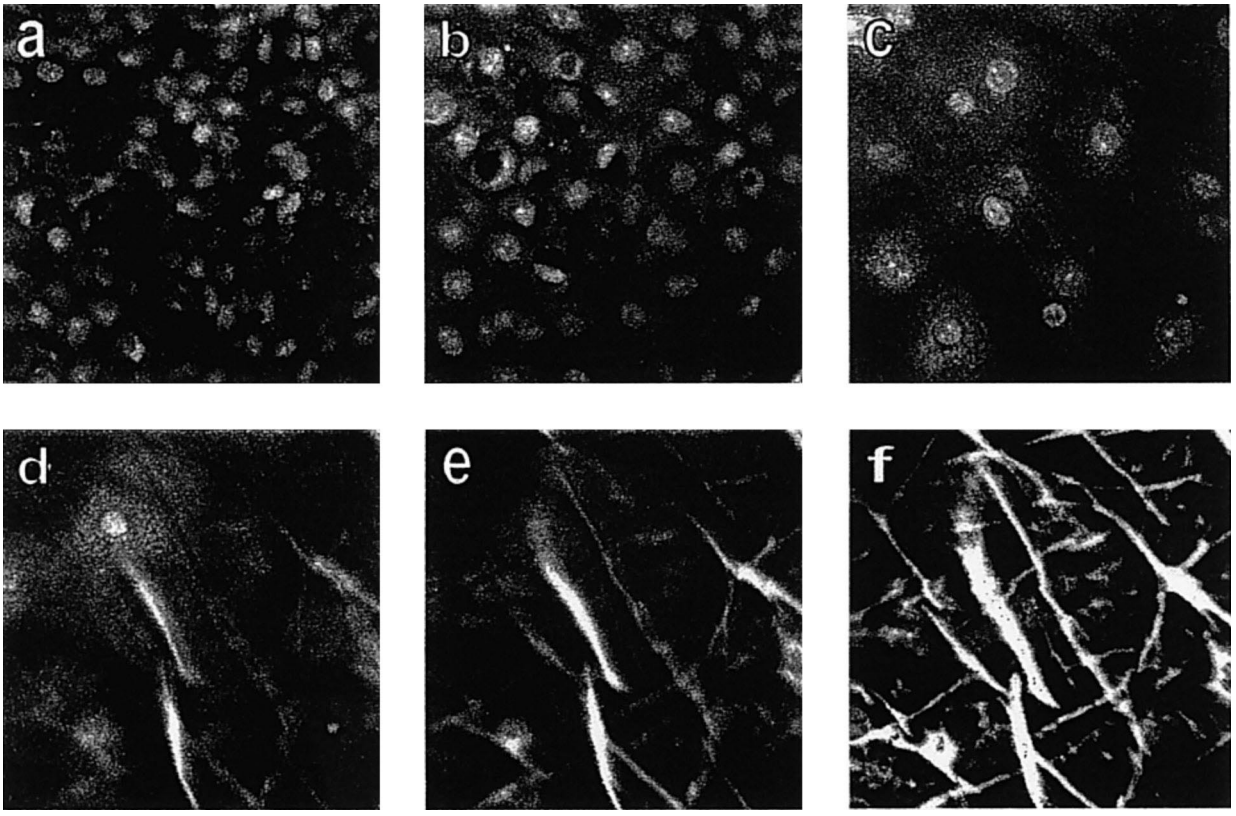

Fig. 9. TPE images of skin treated with PEG-8-L:L-595:CS (70:30:5) liquid-state vesicles and acridine orange for 1 h. *xy*-Images (95×95 μm^2) were recorded at different depths of skin, from a to f with increasing depth. Image d is close to the stratum corneum–stratum granulosum interface. Thread-like channels are formed in the entire stratum corneum and do not continue further down into the stratum granulosum or stratum spinosum. By staining with acridine orange, the stratum granulosum is visualized and provides an indication of the location of the interface with the stratum corneum. All of the underlying cell layers are stained by acridine orange.

to the surface of human skin, several different types of interactions were observed. For all elastic PEG-8-L containing vesicle formulations that were investigated, we observed similar ultrastructural changes. At the stratum corneum surface, intact vesicles were only observed in wrinkles of the skin; at other sites, vesicles had been rinsed off during fixation and dehydration procedures. Vesicles visualized on the surface appear as lipid droplets, which were either surrounded by electron dense material or contained electron dense spots. In addition, intact vesicles were visualized between the upper cell layers of stratum corneum. The upper 2–3 cell layers of stratum corneum are in the process of desquamation and therefore loosely attached. This is the reason that in these regions intact vesicles are able to migrate in intercellular spaces. The appearance of vesicles was different from those observed in previous studies, in which bilayers of vesicles applied on membranes were clearly visualized [26]. In the present study, elastic vesicles were applied on human skin, which may contain sebaceous lipids, or triglycerides derived from contamination with subcutaneous fat. These surface lipids most likely interact with some of the liquid-state vesicles resulting in the formation of lipid filled aggregates. In addition, other morphological changes were observed: intact oligolamellar vesicles and bilayer stacks were detected between the upper 3–4 cell layers of the stratum corneum. Deeper down in the stratum corneum, no intact vesicles were detected. However, lipid areas with electron dense material were found to be located deeper down in OsO_4 fixed tissue of the stratum corneum and must be derived from vesicle constituents, since stratum corneum lipid lamellae are only visualized after fixation with RuO_4.

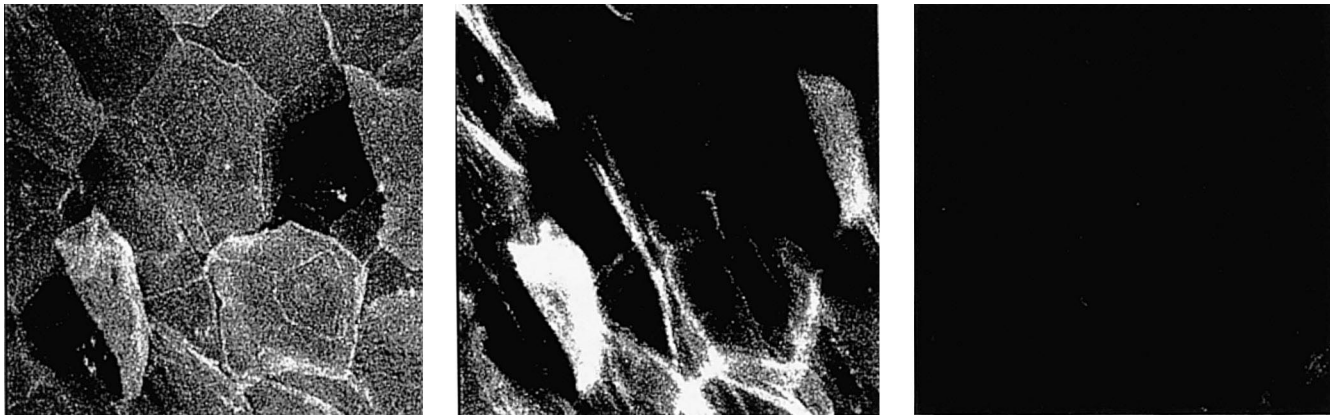

Fig. 10. *xy*-Images at several depths of human skin treated with micelles composed of 100 mol% PEG-8-L. Left panel: 0 μm. Middle panel: −2 μm. Right panel: −5 μm. The polygonal shape of the corneocytes is clearly visualized and fluorescence was detected to a depth of approximately 3 μm in the stratum corneum.

Neither increasing the PEG-8-L content from 30 to 70 mol% nor adding cholesterol sulfate, changed the skin structure modulations induced by vesicles. In addition, no difference in structure modulations was observed in combining the PEG-8-L surfactant with either a saturated C12 surfactant (L-595) or an unsaturated C18 surfactant (EggPC), except for treatment with PEG-8-L:L-595 70:30. Non-occlusive treatment with both L-595:Chol:CS and Wasag-7:Chol:CS rigid vesicles did not affect the skin ultrastructure, which illustrates the importance of the presence of elastic bilayers for ultrastructural changes to occur.

The crystalline state of stratum corneum lipid lamellae and the existence of hydrogen bonds between the head groups and the absence of swelling make that the SC lipid lamellae have a high cohesion. Schreier and Bouwstra [32] supposed that migration of intact vesicles is unlikely to occur. However, Cevc et al. [24,25] postulated that the combination of both

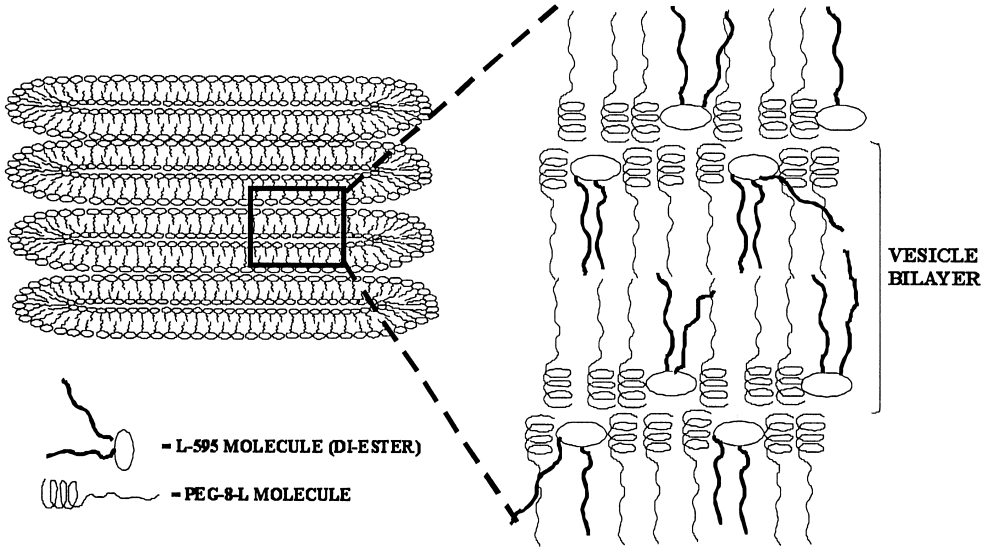

Fig. 11. Schematic overview of lamellar stack formation. Flattened vesicles may fuse together and form bilayer stacks. Possibly the vesicles flatten in the direction in which most easily water will be removed from vesicles, which is most probably water diffusion along the head groups.

elastic vesicles and non-occlusive application should enable vesicles to penetrate through the stratum corneum under the influence of the 'hydration force'. This force should be able to drive elastic vesicles into skin when this force is larger than the resistance when passing intercellular lipid regions in the stratum corneum. The driving force is generated by the hydration gradient across the skin, varying from 15 to 20% in the stratum corneum to 70% in the stratum granulosum. Cevc and Blume claimed that elastic vesicles pass individually through pores in skin [25]. The present TEM results, however, illustrate that our elastic vesicles rather disrupt the stacking of the skin lipid lamellae thereby creating dislocations and possible penetration pathways. In addition, after treatment with PEG-8-L:L-595 (70:30) vesicles, we observed lamellar stacks. The appearance of these stacks might be explained as follows. Under the influence of the hydration force, elastic vesicles partition into the stratum corneum, after which due to the elasticity and reduced water content in the stratum corneum the vesicles might easily flatten. When these flattened vesicles fuse together, bilayer stacks are formed. Since these stacks mainly contain liquid-state bilayers, stacks remain phase separated from the stratum corneum crystalline lipid lamellae. A schematic overview of how such a bilayer stack is illustrated in Fig. 11. Possibly the vesicles flatten in the direction, in which most easily water will be removed from vesicles, which is most probably water diffusion along the head groups. This speculation might justify the perpendicular orientation of bilayer stacks compared to stratum corneum lamellar stacking. Once skin lipid lamellar stacking is disrupted, bilayer stacks are orientated randomly.

However, TEM results did not demonstrate the presence of bilayer stacks after application of both 30 and 70 mol% PEG-8-L:EggPC vesicle formulations. Therefore, further studies are required in order to find out whether stacking of flattened vesicles is facilitated by the linkage of the C12-chains that might be coupled to hydroxy groups located on opposing sides of L-595 sucrose headgroup. In visualization studies with hairless mouse skin, in vivo, similar lamellar stacks were observed after non-occlusive treatment with PEG-8-L:L-595:CS (70:30:5) vesicles, which were orientated perpendicular to skin lamellae or randomly in areas where the skin lamellar organization was disrupted [33]. Additional studies, using, for example, nanogold-labeled surfactants, should be performed to further elucidate the structure and formation of bilayer stacks.

Of course, next to this partitioning of intact vesicles and fusion process in the stratum corneum, it is likely that surfactant molecules are able to diffuse molecularly dispersed through intercellular lipid lamellae and change the lipid organization.

4.2. Freeze-fracture electron microscopy

The FFEM results support the TEM results showing major morphological changes in the intercellular lipid lamellar structure after treatment with PEG-8-L containing elastic vesicles. The large lipid fracture are most probably caused by a decrease in resistance within these areas indicating a less cohesive force between adjacent corneocytes, indicating the effect of the PEG-8-L elastic vesicles on intercellular lipids, whereas the ultrastructure of skin treated with L-595 and Wasag-7 vesicles was not affected. Changes in the viable epidermis ultrastructure could not be observed after treatment with any of the vesicle formulations.

4.3. Two-photon excitation microscopy

The use of fluorescent labeled vesicles alone to elucidate mechanisms by which vesicles interact with human skin is questionable because only the penetration route of the fluorescent marker or its metabolites can be visualized and not the penetration pathways of vesicles. It is, however, excellent technique to study time profiles, penetration pathways and penetration depths of vesicle constituents. As can be seen in Fig. 7, in the absence of vesicles, both acridine orange and fluorescein fail in penetrating into the highly impermeable stratum corneum, as is shown by the presence of a dark 10–20-nm band below the surface. After treatment with fluorescein-DHPE labeled liquid-state vesicles, however, fluorescence is observed within the stratum corneum (Figs. 8 and 9). After an application period of 1 h, the fluorescence extends down into the stratum corneum until the stratum corneum–stratum granulosum interface. Increasing the application period did not show an enhanced penetration depth, which might

imply that dehydration of vesicle formulations on the skin surface is an important factor instead of the application period, for penetration of vesicle constituents into the stratum corneum. The fluorescence of vesicles is always confined to the stratum corneum, even after a 16-h incubation period (not shown). The most apparent observation after treatment with liquid-state vesicles is thread-like channel formation, which are likely to be located within intercellular spaces, since only in the intercellular regions vesicle constituents have been visualized using electron microscopy. These fine thread-like channels could be mistaken for wrinkles in skin; however, the channels reach all the way down into lower parts of the stratum corneum and could not be observed in the stratum granulosum. In addition, these channels were neither observed in skin stained with fluorescein in the absence of elastic vesicles nor in skin treated with micelles (see Fig. 10) and therefore it can be concluded that these elastic vesicles change the penetration pathway of the dye. TEM micrographs of skin occasionally show wrinkles, but they are significantly different since they protrude into the dermis and are considerably larger. Wrinkles such as observed by TEM (see Fig. 2a) are also seen by TPE and appear as bright areas in which fluorescence has accumulated, but have been avoided in the present study when imaging the skin. In other studies, employing confocal laser scanning microscopy, the penetration of amphiphilic fluorescent markers intercalated in vesicle bilayers have been examined as well [6,20]. These studies report of penetration mainly via intercellular routes into the viable epidermis and dermis. In this study, no penetration of fluorescence label into cell layers below the stratum corneum was observed. The studies of van Kuijk-Meuwissen et al. [6] reported a homogeneous distribution of the label in the intercellular space. Cevc et al. [34] proposed the existence of wide clefts between clusters of three to ten corneocytes by which penetration occurs resembling skin wrinkles. However, the appearance of these channels was different from those observed in this study, in which a fine structure of channels is observed localized in the lipid regions within the surface area of only one cell.

The fluorescence of the Wasag-7 rigid vesicles and micelles is restricted to the upper cell layers of the stratum corneum and shows the presence of polygonal shaped corneocytes. No penetration of fluorescent marker was observed below 3–5 μm into the stratum corneum.

5. Conclusions

Elastic vesicles primarily affected intercellular skin lamellae of the stratum corneum. Cell layers below the stratum corneum remained unaffected as was shown by electron microscopy and further supported by the TPE results. Thread-like penetration pathways were visualized by TPE, which were restricted to the stratum corneum and dependent on dehydration of the elastic vesicle formulations rather than application period. The thread-like channels are most likely to be located within intercellular spaces as was shown by TEM and FFEM, which showed modulations of intercellular lipid lamellae. To gain even more insight in the exact mechanisms by which elastic liquid-state vesicles induce ultrastructural changes, other studies, using for example gold labeling techniques could be performed.

Finally, for the topical application of membrane associated drugs, elastic liquid-state vesicles may create or modify penetration pathways in the stratum corneum through which drug molecules can diffuse. Drug molecules could be incorporated in either vesicle bilayers or, in case, the drug molecule change the elasticity and stability of the vesicles, elastic vesicle formulations could be applied prior to application of the drug to induce a penetration enhancement effect.

References

[1] A.S. Breathnach, T. Goodman, C. Stolinski, M. Gross, J. Anat. 114 (1973) 65–81.
[2] P.M. Elias, D.S. Friend, J. Cell Biol. 65 (1975) 180–191.
[3] J.A. Bouwstra, G.S. Gooris, J.A. van der Spek, W. Bras, J. Invest. Dermatol. 97 (1991) 1005–1012.
[4] R.M. Lavker, J. Ultrastruct. Res. 55 (1979) 79–86.
[5] L. Landmann, J. Invest. Dermatol. 87 (1986) 202–209.
[6] M.E.M.J. van Kuijk-Meuwissen, Liposomes and phospholipid/surfactant vesicles. In vitro and in vivo application, Leiden University, The Netherlands, 1998.
[7] P.W. Wertz, D.T. Downing, Science 217 (1982) 1261–1262.

[8] J. Du Plessis, K. Egbaria, N. Weiner, J. Soc. Chem. 43 (1992) 93–100.
[9] V. Gabrijelcic, M. Sentjurc, J. Kristl, Int. J. Pharm. 62 (1990) 75–79.
[10] H.E.J. Hofland, Vesicles as transdermal drug delivery systems, Leiden University, The Netherlands, 1992, p. 162.
[11] H.M. Reinl, A. Hartinger, P. Dettmar, T.M. Bayerl, J. Invest. Dermatol. 105 (1995) 291–295.
[12] K. Egbaria, C. Ramachandran, N. Weiner, Skin Pharmacol. 3 (1990) 21–28.
[13] M.K. Kim, S.J. Chung, M.H. Lee, C.K. Kim, J. Microencapsulation 15 (1998) 21–29.
[14] J. Lasch, R. Laub, W. Wohlrab, J. Control. Release 18 (1991) 55–58.
[15] M. Mezei, V. Gulasekharam, Life Sci. 26 (1980) 1473–1477.
[16] B.A.I. van den Bergh, I. Salomons-de Vries, J.A. Bouwstra, Int. J. Pharm. 167 (1998) 57–67.
[17] H.E.J. Hofland, J.A. Bouwstra, H.E. Bodde, F. Spies, H.E. Junginger, Br. J. Dermatol. 132 (1995) 853–866.
[18] F. Dreher, P. Walde, P. Walther, E. Wehrli, J. Control. Release 45 (1997) 131–140.
[19] A. Rougier, D. Dupuis, C. Lotte, R. Roguet, H. Schaefer, J. Invest. Dermatol. 81 (1983) 275–278.
[20] L. Coderch, M. Oliva, M. Pons, A. delaMaza, A.M. Manich, J.L. Parra, Int. J. Pharm. 139 (1996) 197–203.
[21] M. Kirjavainen, A. Urtti, I. Jääskeläinen, T.M. Suhonen, P. Paronen, R. Valjakka-Koskela, J. Kiesvaara, J. Mönkkönen, Biochim. Biophys. Acta 1304 (1996) 179–189.
[22] H.C. Korting, W. Stolz, M.H. Schmid, G. Maierhofer, Br. J. Dermatol. 132 (1995) 571–579.
[23] D.A. van Hal, Nonionic surfactant vesicles for dermal and transdermal drug delivery, Leiden University, The Netherlands, 1994.
[24] G. Cevc, in: O. Korting, H.C. Braun-Falco, H.I. Maibach (Eds.), Liposomes Dermatics, Springer, Verlag, 1992, pp. 82-90.
[25] G. Cevc, G. Blume, Biochim. Biophys. Acta 1104 (1992) 226–232.
[26] B.A.I. Van den Bergh, Elastic liquid state vesicles as a tool for topical drug delivery, Thesis, Leiden University, The Netherlands, 1999, pp. 49–63.
[27] A.J. Baillie, A.T. Florence, L.R. Hume, G.T. Muirhead, A. Rogerson, J. Pharm. Pharmacol. 37 (1985) 863–868.
[28] B.A.I. van den Bergh, D.C. Swartzendruber, A. Bos-van der Geest, J.J. Hoogstraate, A.H.G.J. Schrijvers, H.E. Boddé, H.E. Junginger, J.A. Bouwstra, J. Microsc. 187 (1997) 125–133.
[29] B.P. Holman, F. Spies, H.E. Boddé, J. Invest. Dermatol. 94 (1990) 332–335.
[30] J.M. Vroom, Two-photon excitation fluorescence lifetime imaging: development and biological applications, University of Utrecht, 1998.
[31] R.J. Scheuplein, J. Soc. Cosm. Chem. 15 (1964) 111–122.
[32] H. Schreier, J.A. Bouwstra, J. Control. Release 30 (1994) 1–15.
[33] B.A.I. Van den Bergh, J.A. Bouwstra, H.E. Junginger, P.W. Wertz, J. Control. Release, in press.
[34] G. Cevc, G. Blume, A. Schatzlein, D. Gebauer, A. Paul, Adv. Drug. Deliv. Rev. 18 (1996) 349–378.